International Journal of Biological Macromolecules 262 (2024) 130137

Contents lists available at ScienceDirect

International Journal of Biological Macromolecules

journal homepage: www.elsevier.com/locate/ijbiomac

Upgrading pectin methylation for consistently enhanced biomass enzymatic saccharification and cadmium phytoremediation in rice *Ospmes* site-mutants

Yanting Wang [a,b,1], Jiaxue Wen [b,1], Sufang Li [b], Jiaying Li [b], Hua Yu [a,b], Yunong Li [b], Xifeng Ren [b], Lingqiang Wang [b], Jingfeng Tang [a], Xin Zhang [c], Zhongqi Liu [c], Liangcai Peng [a,b,*]

[a] *Key Laboratory of Fermentation Engineering (Ministry of Education), National "111" Center for Cellular Regulation & Molecular Pharmaceutics, Cooperative Innovation Center of Industrial Fermentation, Ministry of Education & Hubei Province, Hubei Key Laboratory of Industrial Microbiology, Hubei University of Technology, Wuhan 430068, China*

[b] *Biomass & Bioenergy Research Centre, College of Plant Science & Technology, Huazhong Agricultural University, Wuhan 430070, China*

[c] *Key Laboratory of Original Agro-Environmental Pollution Prevention & Control, Agro-Environmental Protection Institute, Ministry of Agriculture & Rural Affairs, Tianjin 300191, China*

ARTICLE INFO

Keywords:
Biomass porosity
Cellulose accessibility
Alkali pretreatment
Cd removal
Gene editing

ABSTRACT

Crop straws provide enormous biomass residues applicable for biofuel production and trace metal phytoremediation. However, as lignocellulose recalcitrance determines a costly process with potential secondary waste liberation, genetic modification of plant cell walls is deemed as a promising solution. Although pectin methylation plays an important role for plant cell wall construction and integrity, little is known about its regulation roles on lignocellulose hydrolysis and trace metal elimination. In this study, we initially performed a typical CRISPR/Cas9 gene-editing for site mutations of *OsPME31*, *OsPME34* and *OsPME79* in rice, and then determined significantly upgraded pectin methylation degrees in the young seedlings of three distinct site-mutants compared to their wild type. We then examined distinctively improved lignocellulose recalcitrance in three mutants including reduced cellulose levels, crystallinity and polymerization or raised hemicellulose deposition and cellulose accessibility, which led to specifically enlarged biomass porosity either for consistently enhanced biomass enzymatic saccharification under mild alkali pretreatments or for cadmium (Cd) accumulation up to 2.4-fold. Therefore, this study proposed a novel model to elucidate how pectin methylation could play a unique enhancement role for both lignocellulose enzymatic hydrolysis and Cd phytoremediation, providing insights into precise pectin modification for effective biomass utilization and efficient trace metal exclusion.

1. Introduction

Plant cell walls represent the most lignocellulose resources that are transformable for biofuels and biochemicals [1–3]. In higher plants, there are two types of cell walls: a pectin-rich primary cell wall that encircles growing cells and a lignin-high secondary cell wall that upholds structural support to mature cells [4–6]. Particularly, the primary cell wall synthesis involves in cell division and elongation, whereas the secondary cell wall deposition initiates with cell differentiation and thickness [7,8]. As pectin is the most complex polysaccharide rich at galacturonic acid, it plays a regulation role in plant growth and development for biomass production [9,10]. While recent solid-state NMR detections indicate that pectic polysaccharides form a macromolecular network within plant cell walls through covalent interactions and other cross-links [9,10], it suggests that pectic molecules are highly substituted with side chains interlinked with cellulose microfibrils and hemicelluloses, leading to a coextraction of wall polymers from biomass pretreatments [7,11,12]. However, much remains unknown about the pectin modification such as pectin methylation could affect lignocellulose destruction and biomass enzymatic saccharification.

* Correspondence author at: Biomass & Bioenergy Research Centre, College of Plant Science & Technology, Huazhong Agricultural University, Wuhan 430070, China.
E-mail address: lpeng@mail.hzau.edu.cn (L. Peng).
URL: https://bbrc.hzau.edu.cn (L. Peng).
[1] The authors contributed equally

https://doi.org/10.1016/j.ijbiomac.2024.130137
Received 10 October 2023; Received in revised form 9 January 2024; Accepted 11 February 2024
Available online 12 February 2024

Pectin methyl-esterases (PME) proteins have been characterized as the enzymes for catalysis of galacturonic acid de-methylation in plants [4,13], and they are thus considered to play important roles in loosening and stiffening of plant cell walls by demethylesterification of homogalacturonans (HGs) in most plant species [10,14]. Because the uronic acids of pectin are involved in chemical interaction with trace metals [15–20], it remains to explore pectin methylation impact on trace metal accumulation in plant cell walls. Meanwhile, as phytoremediation has drawn attention for trace metal elimination [21–23], genetic engineering of plant cell walls in desirable crops is increasingly thought as a green-like de-toxic technology for exclusion of cadmium (Cd) [24–27], which is one of major trace metals polluted in agricultural lands around the world [19,23,28,29].

As the initial step, physical and chemical pretreatments have been conducted to enhance sequential biomass enzymatic saccharification [30]. For instance, alkali pretreatments are broadly applied to effectively detach hemicellulose with lignin co-extraction [31], which could degrade lignocellulose recalcitrance to improve cellulose accessibility for high enzymatic saccharification in bioenergy crops [32,33]. However, due to its natural recalcitrance, lignocellulose substrates mostly necessitate alkali pretreatments at heavy concentration and high temperature, which not only causes an overpriced biomass process, but also circulates secondary wastes into the environment [34]. Therefore, genetic improvement of lignocellulose recalcitrance has been advanced by selecting genetic mutants and transgenic lines in bioenergy crops.

Rice is one of major food crops over the world and provides large amounts of lignocellulose-rich straw [35,36]. In this study, we initially selected three types of genetic-stable homozygous site-mutants by performing classic CRISPR/Cas9 editing for *OsPME31*, *OsPME34* and *OsPME79* genes in rice wild type/WT (Nipponbare/NPB). Using younger seedlings rich at pectin, we then detected either significantly higher degrees of pectin methylation or much raised biomass porosity in three rice mutants (*Ospme31*, *Ospme34, Ospme79*), compared to their WT. Further performing mild alkali pretreatments with both young rice seedlings and mature straws, this study determined consistently enhanced hexoses yields released from enzymatic hydrolyses of pretreated lignocelluloses in three mutants, mainly due to their augmented cellulose accessibility. Meanwhile, despite of reduced uronic acids levels, this study found that three mutants could accumulate much more soluble Cd in the young seedlings relative to the WT, suggesting a novel mechanism that is different from the previous report about the Cd phytoremediation. Therefore, this study provided a new strategy for enhancing biomass enzymatic saccharification and Cd phytoremediation by upgrading pectin methylation in bioenergy crops.

2. Materials and methods

2.1. Rice mutant selection and biomass sample collection

The rice cultivar (NBP), *Oryza sativa L. japonica*, was used as WT for genetic transformation to generate transgenic rice mutants. The CRISPR/Cas9 editing vector pRGEB32 (donated by Professor Xie Kabin) and CRISPR/Cas9 vector (provided by Mrs. Hu Shiping) were applied for gene-editing of three rice *OsPME31, OsPME34* and *OsPME79* (LOC_Os10g26680, LOC_Os06g09340, LOC_Os01g65790). TBtool was used for gene structure analysis and MEME software was applied to predict the motifs in OsPME protein sequences [37]. Gene transformation and genetic identification of three mutants (*Ospme31, Ospme34, Ospme79*) were accomplished according to our recently-established methods [2,15,38,39].

Rice mutants and WT were grown in the experimental fields of Huazhong Agricultural University, and major agronomic traits were observed as described [38]. The mature rice straws were harvested, dried at 50 °C and stored in a dry container until in use [22]. Meanwhile, the rice seedlings were grown at hydroponics culture for 30 days, and their straws samples were also collected as just described.

2.2. Hydroponic culture of rice seedlings with cd

Rice seeds were germinated in distilled water for 3 days at room temperature, and then shifted into water-culture plates to grow for 15 days within green house at 26 °C. Every two days, the culture plates were slightly shaken and supplemented with water to the initially-fixed levels. The 15-day-old seedlings were further supplied with 200 μM $CdCl_2$ (CAS No.10108–64-2) to grow for another 15 days under regular shaking and water supplement as described just. All 30-day-old seedings materials were collected for determination of total Cd and phosphate-buffer-extractable Cd as previously described [15,40]. Each treatment contained 96 rice seedlings with three biological duplications.

2.3. Wall polymer extraction and determination

Wall polysaccharides of biomass samples were extracted as previously described [41]. The soluble sugars, lipid and starch were consequently separated by phosphate buffer (pH 7.0), chloroform–methanol (1:1, *v*/v) and dimethyl sulphoxide (DMSO)–water (9:1, v/v) [42]. The remaining crude cell walls were suspended in 0.5 % (*w/v*) ammonium oxalate (5.0 ml) and heated for 1 h in a boiling water bath and all supernatants were used as pectin samples. The remaining pellets were extracted with 4 M KOH containing $NaBH_4$ (1.0 mg/mL) and the combined supernatants were collected as KOH-extractable hemicellulose fraction. The residues were suspended in 67 % H_2SO_4 (*v*/v) for 1 h at 25 °C to determine hexoses accounting for cellulose levels. Total hemicelluloses were calculated subjective to hexoses and pentoses in the KOH-extractable hemicellulose fraction and pentoses in the remained cellulose pellets. UV-VIS spectrometer (V—1100D, Shanghai MAPADA Instruments Co.) was employed for hexose, pentose and uronic acids assays as previously described [43]. All experimental analyses were completed under independent triplicate.

2.4. Pectin methylation assay

For measurement of pectin methylation degree [15], pectin was initially extracted with ammonium oxalate solution as described above, and I mL pectin solution was incubated with 0.4 mL of 0.5 M NaOH for 1 h at room temperature. After neutralization with 0.2 mL of 1 M HCl, the pectin sample was centrifuged at 2400*g* for 10 min, and the released methanol was oxidized for 15 min at room temperature using 0.03 units of alcohol oxidase (Sigma-Aldrich; www. sigmaaldrich.com) in 0.25 mL of 20 mM phosphate buffer (pH 7.5). The resultant extract was then treated for 15 min at 60 °C in 20 mM acetyl acetone, 50 mM acetic acid, and 2 M ammonium acetate. Absorbance was read at 412 nm and a standard curve was generated with a methanol dilution series for calculation of pectin methylation degree. All assays were completed at independent triplicate.

2.5. Immunolabeling observation of wall polysaccharides

Rice stem (0.5–1.0 cm) tissues were embedded with 4 % agar, cut into 80 μm sections using a microtome (VT1000S, Leica) [44], and then embedded in paraplast plus for immunolabeling as described [15,30]. Sections were rinsed completely in PBS buffer, incubated with 5-fold dilution of cell wall glycan-directed monoclonal antibodies (mAbs) followed by 200-fold and 100-fold dilution of anti-mouse IgG linked to fluorescein isothiocyanate (FITC). LM-19 and LM-20 were applied to recognize epitopes in de-esterified homogalacturonan. After section samples were well rinsed, the FITC fluorescence was observed with an confocal microscopy (Olympus FV1200) equipped with epifluorescence optics as previously described [30].

2.6. Measurement of cellulose crystallinity, polymerization and accessibility

Cellulose crystalline index (CrI) was detected by Rigaku-D/MAX instrument (Ultima III, Japan) as previously described [15,45]. The biomass sample was laid on the glass holder (35 × 50 × 5 mm) and examined under plateau conditions. Ni-filtered Cu Kα radiation (λ = 0.154056 nm) generated at voltage of 40 kV and current of 18 mA, and scanned at speed of 0.0197°/s from 10° to 45°. The crystallinity index was calculated using the intensity of the 200 peak (I200, θ = 22.5°) and the intensity at the minimum between the 200 and 110 peaks (Iam, θ = 18.5°) as the following equation: CrI = 100 × (I200–Iam)/I200.

The viscosity method was previously described [15] to detect the degree of polymerization (DP) of cellulose samples according to the equation: $DP^{0.\ 905} = 0.\ 75\ [\eta]$. The [η] is the intrinsic viscosity of the solution, and all experiments were performed at 25 ± 0.5 °C using an Ubbelohde viscosity meter and cupriethylenediamine hydroxide (Cuen) as the solvent. The intrinsic viscosity was calculated using the USP table (USP, 2002) that lists the predetermined values of the product of intrinsic viscosity and concentration.

Congo red (CR) stain was applied to estimate cellulose accessibility as previously described [32,46,47]. The samples (100 mg) were treated with a series of CR solutions (0.50, 1.0, 2.0, 4.0, 6.0, 8.0 mg/mL) in 0.3 M phosphate buffer (pH 6) with 1.4 mM NaCl at 60 °C for 24 h. After centrifugation at 4000*g*, the absorbance of the supernatant was measured under 498 nm and the maximum amount of adsorbed dye was calculated by subtraction of free dye in the supernatant from the initial dye. The dye adsorption capacity was estimated between the initial added dyes and the final free dyes in the supernatants using equation: Ae = (Ci – Ce) x V/(M x 1000). All measurements of cellulose DP and CR values were conducted in independent triplicates.

2.7. Fourier transform infrared (FTIR) spectroscopy and scanning electron microscopy (SEM) observation

FTIR spectroscopy was applied to scan rice biomass samples using Perkin-Elmer Ppectro-photometer (NEXUS 470, Thermo Fisher Scientific, Waltham, MA, USA) as previously described [38,48]. The biomass morphology was observed under SEM (SEM JSM-IT300, Akishima, Tokyo, Japan) as described [49]. Well-mixed biomass samples were sputter-coated with gold in a JFC-1600 ion sputter (Mito City, Japan) and visualized for 5–8 times to acquire representative images.

2.8. Biomass pretreatment and enzymatic hydrolysis

For alkali pretreatments, biomass samples were treated with NaOH (0.25 %, 1 %, *w/v*) at 50 °C for 2 h under 150 rpm shaken as previously described [41]. After centrifugation at 3000 *g* for 5 min, the pellets were washed with 10 mL distilled water until pH 7.0, and then incubated with the final concentration of 1.6 g/L mixed-enzymes (cellulases: 10.6 FPU/g biomass; xylanases: 6.72 U/g biomass purchased from Imperial Jade Biotechnology Co., Ltd), while co-supplied with 1 % Tween-80 as described [48]. The hexoses yield was estimated according to the following equation: Hexoses yield (%) = hexoses released (g) x 100/cellulose content (g), whereas the total sugars yield was based on the equation: Total sugars yield (%) = total hexoses and pentoses released (g) x 100/dry matter content (g). All experiments were accomplished under independent triplicate.

2.9. Detection of cd levels in rice seedlings

The dry seedings and phosphate-extracted solution were respectively added into the porcelain crucible and transferred to the muffle furnace for determining total Cd and soluble Cd levels. The temperature of muffle furnace was gradually raised to 200 °C for 30 min, and fixed at 600 °C for 6–8 h. The ashes were dissolved with 1.0 % HNO_3 (*v*/v), washed with 1.0 % HNO_3 for 3 times, and all solutions were collected into a 25 mL volumetric flask. An atomic absorption spectrometer (Agilent 240Z GFAA) was applied to detect Cd content as previously described [15]. All samples were measured under independent triplicate.

2.10. Statistical analysis

Superior Performance Software Systems (SPSS version 17.0, Inc., Chicago, IL) was applied for statistical calculation. Correlation coefficients were completed by Spearman's rank for all measured parameters. Pair-wise comparisons were based on Student's *t*-test as described.

3. Results and discussion

3.1. Site mutations of OsPME31, OsPME34 and OsPME79 involved in pectin methylation

As PME enzymes involve in catalysis of galacturonic acid methylation in pectic polysaccharides [4,13], this study applied classic CRISPR/Cas9 gene-editing system with rice WT to perform site mutations of *OsPME31*, *OsPME34* and *OsPME79*, which are three representative genes of rice OsPMEs family (Fig. 1 A). Using our previously-established approach [38,50], this study identified three homozygous mutants termed as *Ospme31*, *Ospme34* and *Ospme79* (Fig. 1 B). As a comparison with WT, the *Ospme31* and *Ospme34* mutants showed a single amino acid alteration, whereas the *Ospme79* mutant was of single amino acid deletion (Fig. 1 C). Meanwhile, three mutants were checked without the occurrence of the off-target mutations, suggesting that all mutants were of genetic stability. Although three mutants showed significantly reduced plant heights by 6 %–15 % at $p < 0.01$ levels ($n = 3$), they all had much raised tillers numbers by 22 %–41 % compared to the WT, leading to similar dry biomass yields examined between the *Ospme31* and *Ospme34* mutants and WT in the field experiment (Table S1). Exceptionally, the *Ospme79* mutant had significantly higher dry biomass weight than that of the WT by 20 % at $p < 0.05$ level (n = 3). Hence, site mutations of *OsPME*s genes should be applicable to select the desirable mutants for function analysis of OsPMEs enzymes involved in pectin methylation in plant cell walls. However, it remains to test the dry weights of mature straws and seed yields of three mutants on large scale in the future.

3.2. Reduced pectin level and altered lignocellulose composition in young seedlings of three Ospmes mutants

Because pectic polysaccharides are rich at primary cell walls in higher plants [51,52], this study performed hydroponic culture to collect young seedlings of three rice *Ospmes* mutants and WT (Fig. 2 A). As a difference from mature rice straws, the young seedlings of three mutants showed their plant heights similar to the WT. However, despite of a normal plant growth in the young seedlings, three mutants were examined with significantly reduced pectin levels by 12 %–23 % at $p < 0.05$ and 0.01 levels ($n = 3$), compared to the WT (Fig. 2 B). Meanwhile, significantly reduced cellulose contents were detected by 20 %–23 % in three mutants, but their hemicelluloses levels were much raised by 22 %–60 %, compared to the WT. As primary cell walls make up relatively high biomass proportions at young seedlings [15,30], such enhanced hemicellulose deposition should compensate for inhibited pectin and cellulose biosynthesis to maintain plant cell wall integrity and normal plant growth as observed above, which may also explain why similar dry biomass yields were estimated in mature rice straws of three mutants and WT.

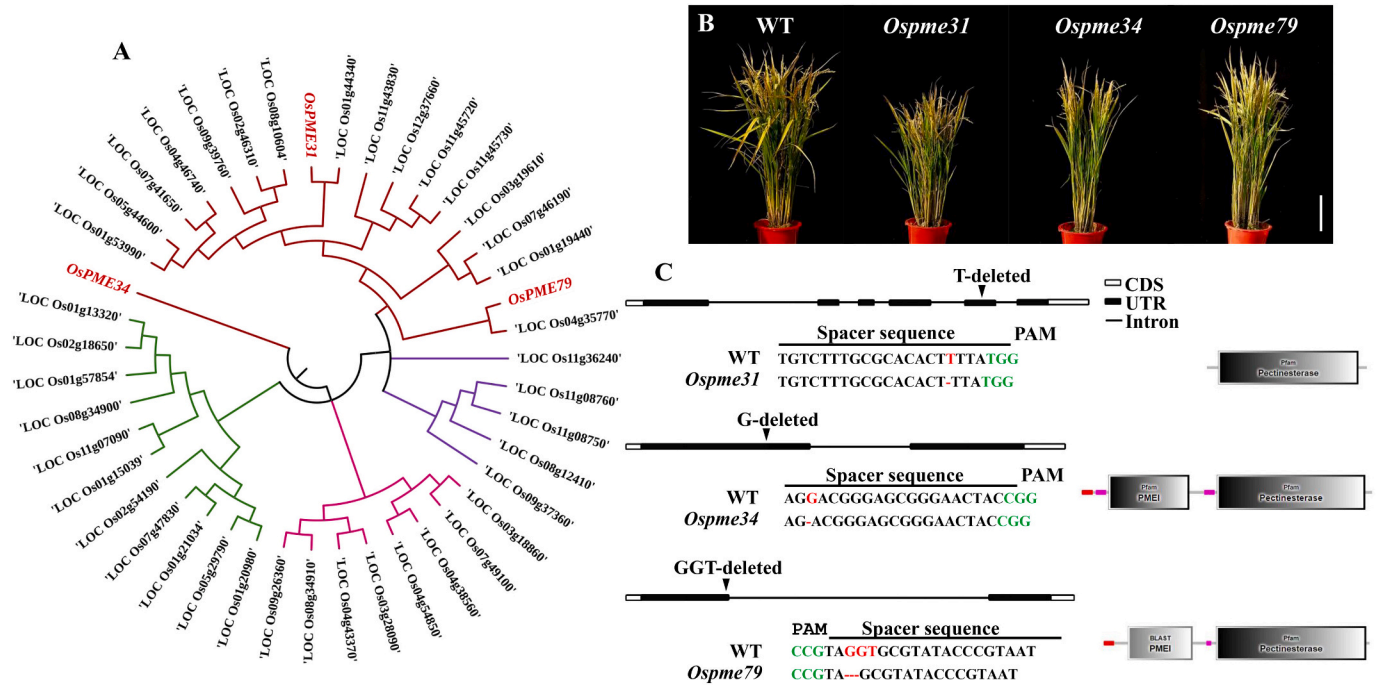

Fig. 1. Characterization of rice *OsPMEs* family and three *Ospme* mutants generated by CRISPR/Cas9 editing. (A) Phylogenic tree of *OsPMEs* genes; (B) Images of mature plants of three *Ospmes* mutants and wild type/WT (NPB), scale bar as 20 cm; (C) Mutation sites of three *Ospmes* mutants by CRISPR/Cas9 editing. Cd accumulation with lignocellulose tissues of rice mutant (*Osfc16*) and WT (NPB).

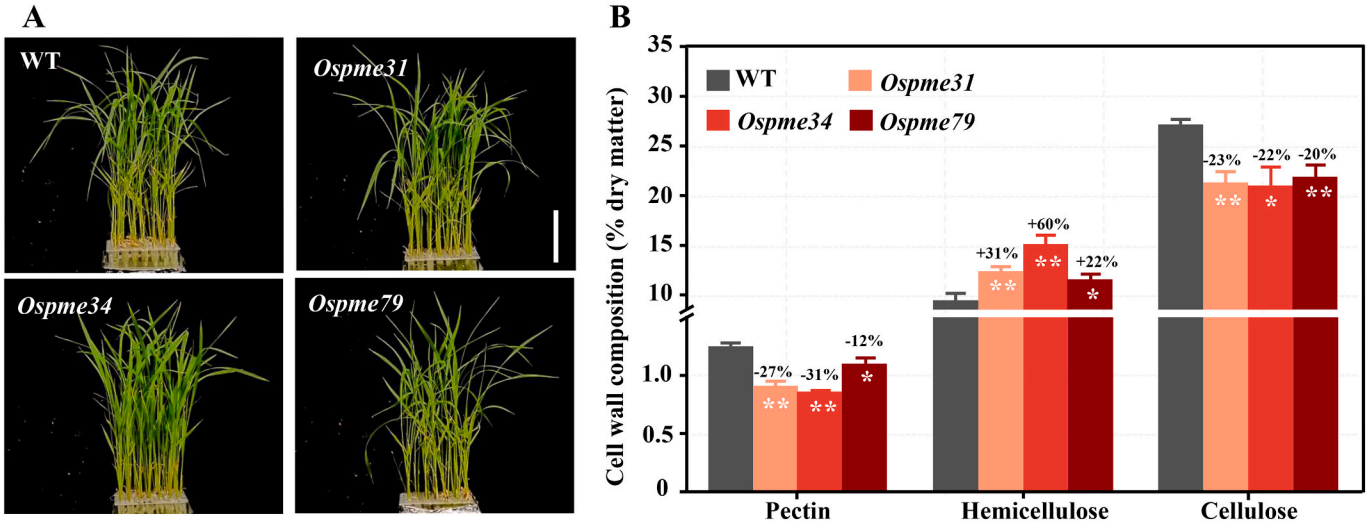

Fig. 2. Cell wall composition of young seedlings in rice mutants and WT from hydroponic culture. (A) Images of 30-day-old seedlings, scale bar as 5 cm; (B) Wall polymer levels; * And ** as significant difference by *t*-test between the mutant and WT at $p < 0.05$ and 0.01 levels ($n = 3$), respectively; # The percentage value calculated by subtraction between mutant and WT divided by WT.

3.3. Significantly upgraded pectin methylation degree in seedlings of three mutants

With respect to their pectin levels reduced in young rice seedlings, this study detected significantly lower uronic acids contents in three mutants than those of the WT by 14 %–32 % at $p < 0.01$ levels (Table 1). By performing typical pectin methylation assay *in vitro* [30,53], this work determined significantly raised methanol levels by 7 %–21 % in young seedlings of three mutants, which estimated pectin methylation degrees upgraded by 29 %–73 % in three mutants relative to the WT. To confirm pectin methylation degrees upgraded in three mutants as examined *in vitro*, we attempted to *in situ* observe immunofluorescent distribution by using the LM20 and LM19 antibodies that are specifically against high- and low-methylated HGs in plant cell walls of stem tissues (Fig. 3 A). Based on semi-quantitation of immunofluorescent images, this study calculated either much raised immunofluorescent intensity for highly-methylated HGs by 27 %–44 % or significantly reduced intensity for lowly-methylated HGs by 16 %–37 % in three mutants, compared to the WT (Fig. 3 B). Therefore, the data indicated that the site mutations of three *OsPMEs* could consistently raise the methylation degrees of HGs in plant cell walls of three rice mutants. On the other hands, this study has thus provided dual evidences *in vitro* and *in situ* to confirm that the three OsPMEs are of enzymatic activities for catalysis of pectin de-methylation in plants [4,14].

Table 1
Pectin methylation degrees of young seedlings among three *Ospme* mutants and WT.

Sample	Uronic acids (mg/ml)	Methanol (mg/ml)	Degree of methylation (%)
WT	1.11 ± 0.04	0.29 ± 0.00	25.69 ± 0.35
Ospme31	0.86 ± 0.04 ** (-23 %)[#]	0.35 ± 0.01** (+ 21 %)	41.23 ± 1.10** (+ 60 %)
Ospme34	0.76 ± 0.01** (-32 %)	0.34 ± 0.01* (+ 17 %)	44.40 ± 1.85** (+ 73 %)
Ospme79	0.96 ± 0.04 ** (-14 %)	0.31 ± 0.01* (+ 7 %)	33.05 ± 0.49** (+ 29 %)

* And ** as significant difference by *t*-test between the mutant and WT at $p < 0.05$ and 0.01 levels ($n = 3$), respectively.
[#] The percentage value calculated by subtraction between mutant and WT divided by WT.

3.4. Distinctively elevated biomass porosity in seedlings of three mutants

Although pectin methylation is considered to regulate loosening and stiffening of plant cell walls [54], little is known about its impact on biomass porosity. In this study, we examined biomass porosity in three mutants and WT by performing characteristic BET analysis of N2 adsorption/desorption [55]. In terms of the raw materials of young seedlings, the *Ospme31* and *Ospme79* mutants exhibited consistently increased pore volumes than those of the WT among pore diameter distributions ranged from 2 nm to 45 nm, whereas the *Ospme34* mutant showed larger volumes only for 2–10 nm pores (Fig. 4 A). Even though pectin removal could increase pore volumes in all samples examined, the *Ospme34* and *Ospme79* mutants remained larger pore volumes than those of the WT from 2 nm to 45 nm pore distributions, and the *Ospme31* mutant was of raised volumes only from 2 nm to 10 nm pores (Fig. 4 B). Meanwhile, all three mutants, compared to the WT, exhibited much more raised volumes from 2 nm to 10 nm pores, but distributions of the raised pore volumes were varied among three mutants examined.

Furthermore, this study estimated three major parameters accountable for average values of BET surface area, pore volume and pore size (Table 2). As a result, the *Ospme79* mutant showed mostly increased surface areas and pore volumes than those of the WT by 46 %–81 % in both raw materials and pectin-extracted (de-pectin) lignocellulose samples, whereas the *Ospme31* mutant had the surface areas and pore volumes raised by 12 %–33 %. By further comparison, the *Ospme34* mutant was of slightly raised surface areas and pore volumes by 1 %–12 %. Notably, all three mutants appeared to have much reduced pore sizes than those of the WT by 17 %–45 %, which suggested that the biomass porosity increased in three mutants should be due to much more nanopores occurrence in plant cell walls.

3.5. Consistently enhanced biomass enzymatic saccharification in seedlings and mature straws

Since biomass porosity is accountable for biomass enzymatic saccharification examined in diverse bioenergy crops [19,32,49,56], this study determined both hexoses (% cellulose) and total sugars (hexoses and pentoses) yields released from enzymatic hydrolyses of alkali-pretreated young seedlings in three mutants and WT (Fig. 5). By performing NaOH pretreatments at low concentrations (0.25 %, 1 %), we examined significantly enhanced hexoses yields (% cellulose) by 22 %–53 % at $p < 0.01$ levels ($n = 3$) in three rice mutants, compared to the WT (Fig. 5 A). In particular, the *Ospme34* mutant could achieve a near-complete biomass enzymatic saccharification with hexoses yield of 97 %

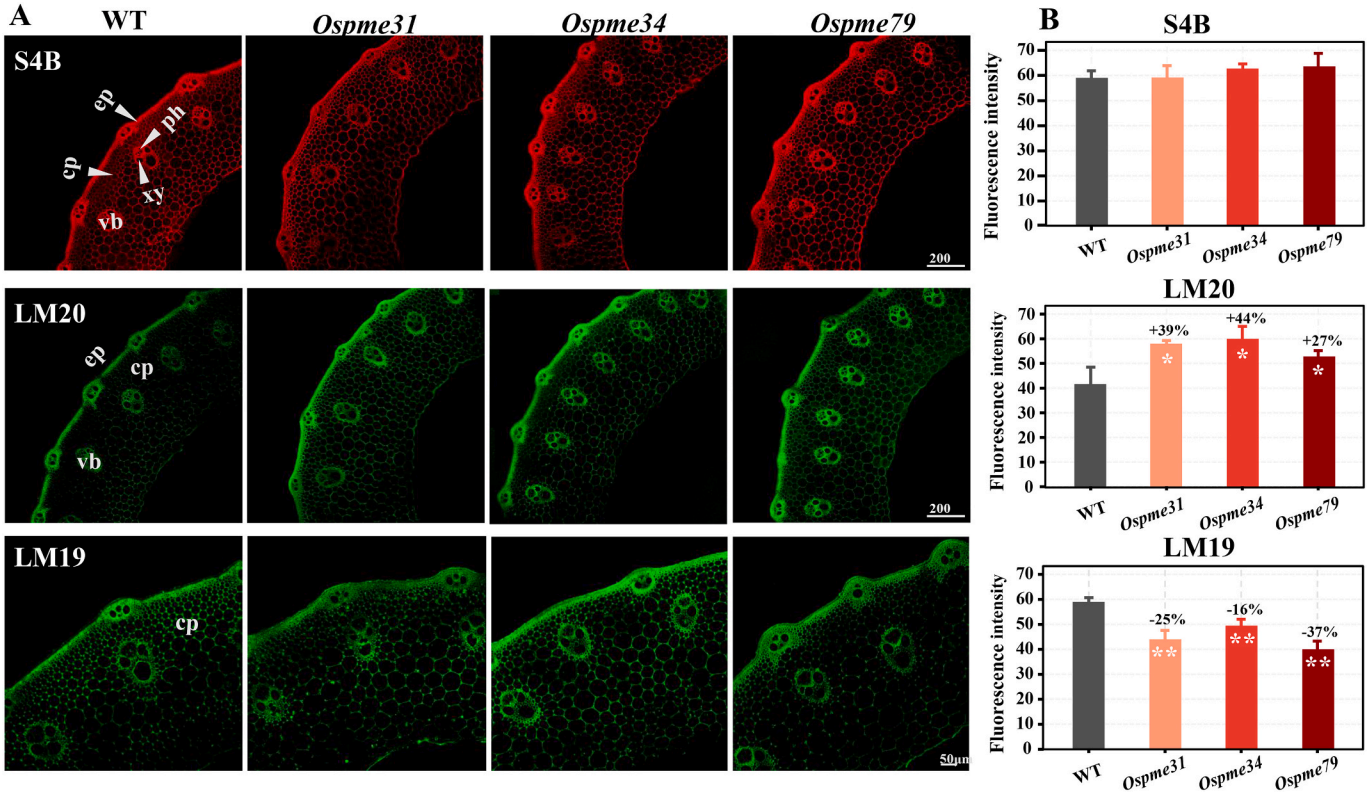

Fig. 3. Immunofluorescent labeling of pectin (HG) epitopes in transverse stem sections (80 nm thick) of young seedlings in rice mutants and WT. (A) Representative immunofluorescent images recognized by either LM20 and LM19 antibodies against for high- and low-methylated HGs or S4B dye specific for cellulose staining; (B) Semi-quantitation of histological staining and immunofluorescent images by using ImageJ; * And ** as significant difference by *t*-test between the mutant and WT at $p < 0.05$ and 0.01 levels ($n = 3$), respectively; [#] The percentage value calculated by subtraction between mutant and WT divided by WT; ep (epidermis), cp: cortical parenchyma, vb (vascular bundle), Xy (xylem), ph (phloem), gc (guard cells).

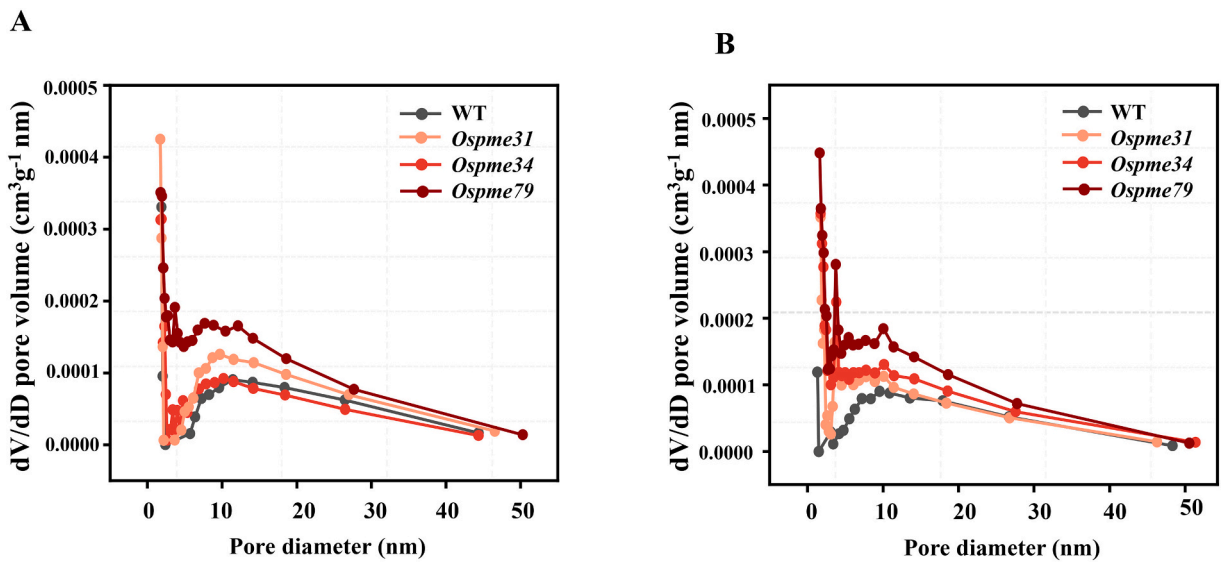

Fig. 4. Biomass porosity of young seedlings in rice mutants and WT from BET analyses. (A) Raw materials; (B) Lignocellulose substrates after pectin extraction of young seedlings with 0.5 % ammonium oxalate.

Table 2
Biomass porosity of young seedlings by BET analysis in rice mutants and WT.

Sample	BET surface area (m^2/g)		Pore volume (mm^3/g)		Pore size (m^2/g)	
	Raw material	De-pectin lignocellulose	Raw material	De-pectin lignocellulose	Raw material	De-pectin lignocellulose
WT	1.47	1.61	2.27	2.34	20.10	23.84
Ospme31	1.64 (+12 %)#	1.96 (+22 %)	2.91 (+28 %)	3.12 (+33 %)	16.70 (−17 %)	14.48 (−39 %)
Ospme34	1.50 (+2 %)	1.63 (+1 %)	2.29 (+1 %)	2.61 (+12 %)	15.18 (−24 %)	13.18 (−45 %)
Ospme79	2.37 (+61 %)	2.35 (+46 %)	4.10 (+81 %)	4.03 (+72 %)	14.81 (−26 %)	13.08 (−45 %)

Data were derived from BET analyses as shown in Fig. 4; # The percentage value calculated by subtraction between mutant and WT divided by WT.

(% cellulose) under 1 % NaOH pretreatment. Meanwhile, despite of reduced cellulose levels, three mutants remained to achieve significantly higher total sugars (hexoses and pentoses) yields (% dry matter) than those of the WT at $p < 0.05$ levels (Fig. 5 B), which should be due to efficient cellulose digestion and relatively raised hemicellulose levels in three mutants. Furthermore, although the mature rice straws contain small amounts of primary cell walls [57], this study determined even enhanced biomass enzymatic saccharification in three rice mutants. Compared to the WT, three mutants produced the hexoses and total sugars yields raised by 29 %–63 % under 1 % NaOH pretreatment with mature straws (Fig. 5 C & D), which may be due to the efficient digestion of primary cell walls enabled to consequently facilitate enzymatic saccharification of secondary cell walls in mature rice straws. The results have therefore indicated that biomass enzymatic saccharification could be consistently enhanced in both young seedlings and mature straws of three rice mutants.

3.6. Largely increased Cd accumulation in seedlings of three mutants

By means of our recently-established hydroponic culture [15], this study supplied Cd (200 umol/L) with rice seedlings for 15 days, and then determined Cd accumulation in three mutants and WT (Fig. 6). As a comparison, three rice mutants contained significantly higher Cd levels than those of the WT at $p < 0.01$ levels ($n = 3$) (Table 3). In particular, the *Ospme34* mutant was of the most raised Cd accumulation up to 2.4 fold, compared to the WT. Notably, this study examined much more insoluble Cd accumulation in three mutants than that of the WT by 1–3.5 folds, suggesting that three mutants should mainly accumulate Cd in their plant cell walls. As pectin could play a major role for much Cd accumulation with lignocelluloses by chemical interaction with uronic acids as previously reported [15,20,30], it assumed that three rice mutants should involve in a novel mode for Cd accumulation, based on their reduced pectin levels and raised methylation degrees examined above. On the other hands, such more Cd accumulation in three mutants may be due to their raised hemicellulose levels and enlarged nanopore volumes [2,23].

3.7. Specifically reduced lignocellulose recalcitrance in three mutants

To understand biomass enzymatic saccharification enhanced in seedlings of three rice mutants, this study further determined two major cellulose features (CrI and DP), which are accountable for lignocellulose recalcitrance [32,55,58]. As a result, three rice mutants showed significantly reduced cellulose CrI and DP values than those of the WT at $p < 0.05$ and 0.01 levels in their seedlings tissues (Fig. 7 A & B). In particular, cellulose DP values were much decreased in three mutants by 21 %-34, probably due to inhibited cellulose biosynthesis for less cellulose levels examined above. By further performing Congo red staining with lignocellulose substrates after 1 % NaOH pretreatments, we detected significantly increased cellulose accessibility in three rice mutants by 21 %–26 %, compared to the WT (Fig. 7 C), which has been defined as the parameter directly accounting for biomass enzymatic saccharification [58]. Under fourier transform infrared spectroscopy, we meanwhile observed at least five altered peaks located at 829 cm^{-1} (C—H), 898

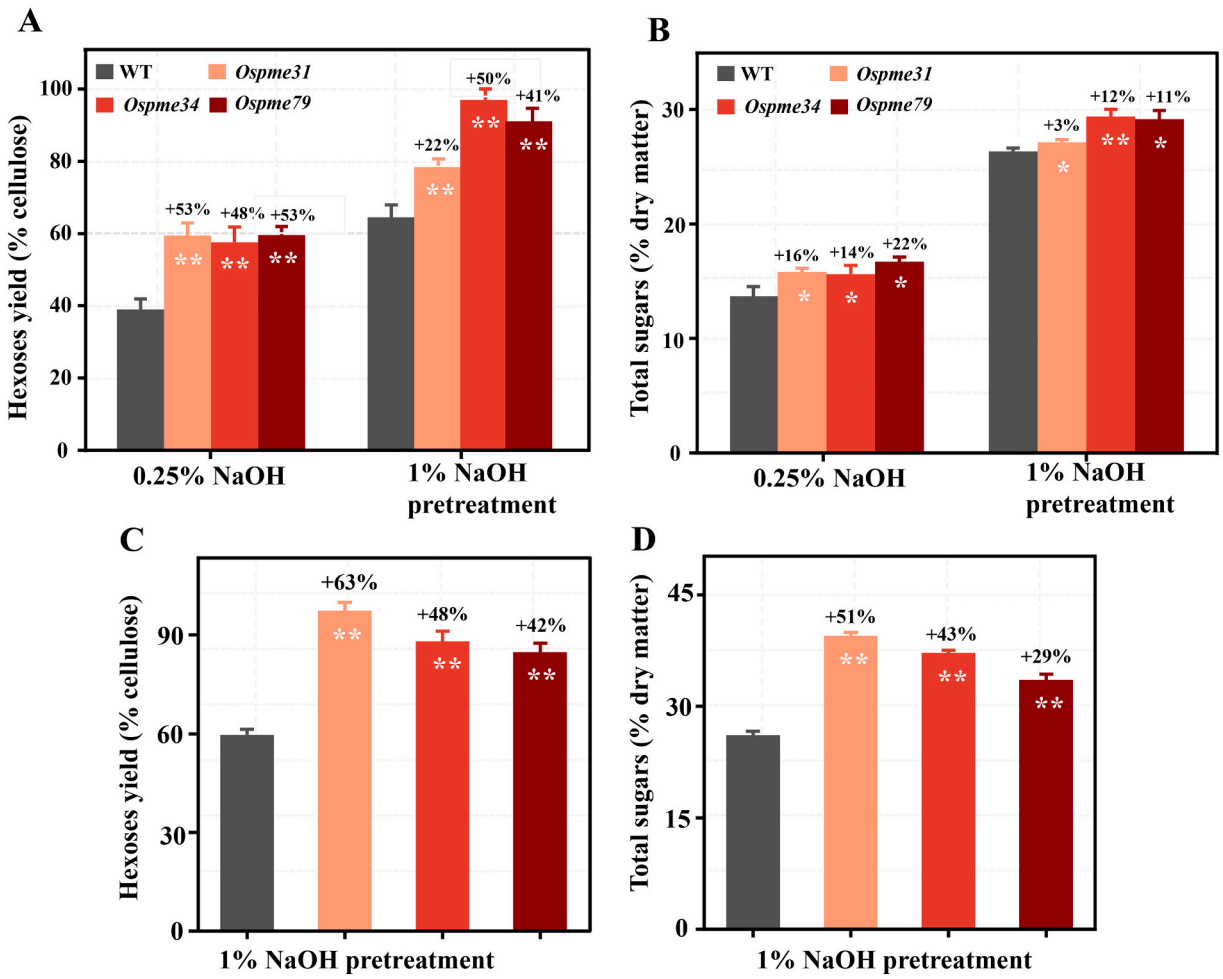

Fig. 5. Biomass enzymatic saccharification of rice mutants and WT upon NaOH pretreatments. (A, B) Hexoses and total sugars (hexoses + pentoses) yields released from enzymatic hydrolyses after 0.25 % and 1 % NaOH pretreatments with young seedlings; (C, D) Hexoses and total sugars yields released from enzymatic hydrolyses after 1 % NaOH pretreatments with mature rice straws; * And ** as significant difference by *t*-test between the mutant and WT at $p < 0.05$ and 0.01 levels ($n = 3$), respectively; # The percentage value calculated by subtraction between mutant and WT divided by WT.

cm^{-1} (C-O-C), 1241 cm^{-1} (C-O-C), 1373 cm^{-1} (C—H), 1509 cm^{-1} (C=C) in the 1 % NaOH-pretreated residues of three mutants (Fig. 8 A), which should be accounting for partial wall polymer extraction and cellulose feature alteration from 1 % NaOH pretreatments. By comparison, the WT only displayed four peaks altered, suggesting its less wall polymer extraction for less cellulose accessibility examined above. Furthermore, we applied scanning electron microscopy (SEM) to observe the surfaces of biomass residues remained from enzymatic hydrolyses of 1 % NaOH pretreated seedlings in the representative *Ospme34* mutant and WT (Fig. 8 B). Notably, the *Ospme34* mutant exhibited grain-like residues, which should be accountable for near-complete cellulose hydrolysis in the mutant as described above. By contrast, the WT remained partial undigestible cellulose microfibrils, consistent with its less biomass enzymatic saccharification examined.

3.8. A hypothetic model about pectin methylation roles in biomass saccharification and Cd accumulation

Based on all data obtained in this study and major findings as previously reported, this study proposed a hypothetic model to explain why three rice *Ospme* mutants were of consistently enhanced biomass saccharification and Cd accumulation (Fig. 9). As pectic polysaccharides are interacted with hemicelluloses *via* chemical linkages of uronic acids [7,11,15,18], this study has thus demonstrated that raised methylation degrees of uronic acids should cause a partial disassociation between pectin and other wall polysaccharides in primary cell walls of three rice mutants, leading to relatively increased hemicellulose deposition. Meanwhile, it is assumed that more hemicellulose deposition may inhibit cellulose synthesis for less cellulose levels examined in three mutants, but it remains interesting to sort out its regulation mechanism in the future. However, it is understandable that much reduced cellulose CrI and DP values should be mainly due to inhibited cellulose biosynthesis and raised hemicellulose in three mutants [23,58]. Because it has been characterized that reduced cellulose DP is accounting for more reducing ends of cellulose microfibrils, this study has examined significantly elevated cellulose accessibility and biomass porosity in three rice mutants [2,55,59]. In addition, hemicellulose disassociation should be another factor for much raised biomass porosity in the mutants. Therefore, this hypothetic model has concluded two major causes accountable for remarkably enhanced biomass enzymatic saccharification in three mutants. Since hemicelluloses are partially substituted by uronic acids [20], the model has also indicated two major factors for increased Cd accumulation in the mutants, suggesting a novel mechanism for Cd phytoremediation by upgrading pectin methylation in plants.

To simply understand the hypothetic model that highlights the advantage of this study, we further presented the dynamic alterations of cell walls structures accountable for the major findings achieved in three mutants, thereby indicating its potential applications for multiple fields (Fig. 10). On the other hands, this structure model hints for the

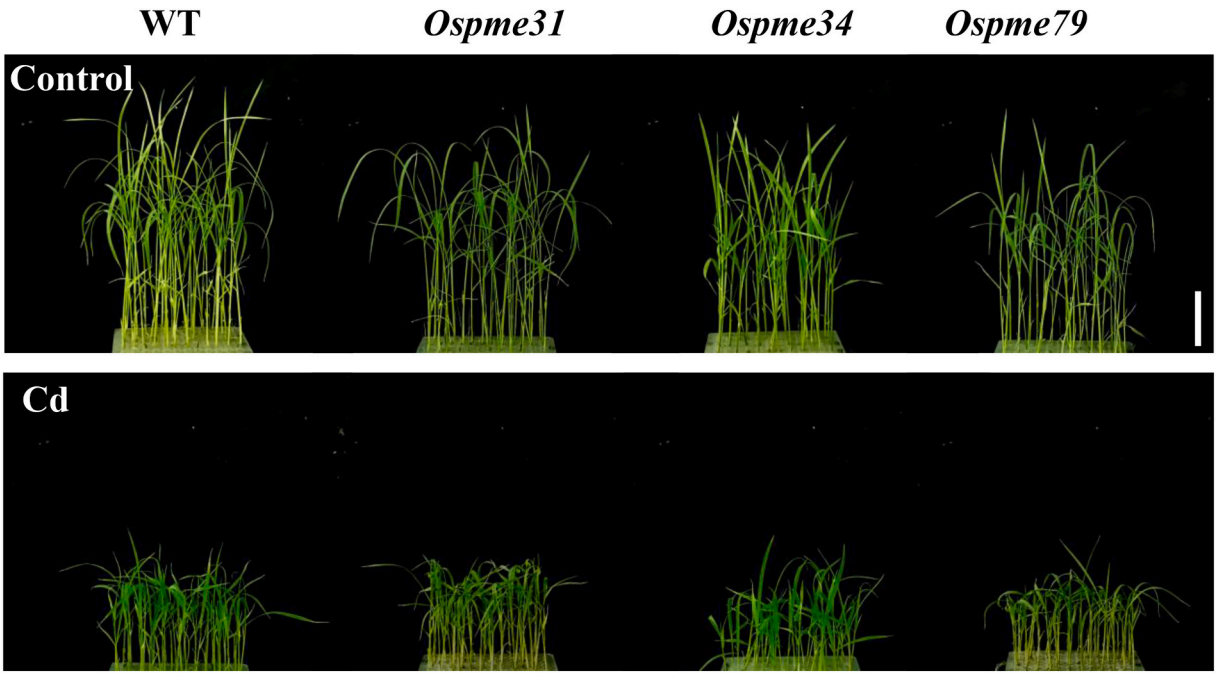

Fig. 6. Images of 30-day-old seedlings in three *Ospme* mutants and WT from hydroponic culture co-supplied with 200 μmol/L cadium. Scale bar as 5 cm.

Table 3
Cd accumulation in young seedlings of *Ospme* mutants and WT from hydroponic culture

Sample	Insoluble Cd (mg/g)	Total Cd (mg/g)
WT	0.13 ± 0.00	0.28 ± 0.00
Ospme31	0.26 ± 0.00** (+100%)[#]	0.35 ± 0.01** (+25%)
Ospme34	0.58 ± 0.04** (+346%)	0.95 ± 0.03** (+239%)
Ospme79	0.42 ± 0.01** (+223%)	0.55 ± 0.01** (+96%)

** As significant difference by *t*-test between the mutant and WT at $p < 0.01$ levels (n = 3); [#] The percentage value calculated by subtraction between mutant and WT divided by WT.

limitation of this study such as in-depth wall polymer interactions. However, as advanced solid-state NMR technology has recently been applied to observe pectin dynamic regulation and interaction for primary cell wall formation [60–64], this study could provide excellent biological samples to explore the specific role of pectin methylation in wall network construction in plants.

4. Conclusion

By performing typical CRISPR/Cas9 editing for *OsPME31*, *OsPME34* and *OsPME79* genes in rice cultivar, this study selected three distinct site-mutants that showed plant growth and biomass yields similar to the WT. However, significantly upgraded pectin methylation degrees were observed in plant cell walls *in situ*, and also determined *in vitro* in young seedlings of three mutants, leading to much improved lignocellulose recalcitrance such as either reduced cellulose level and feature (CrI and DP values) or raised cellulose accessibility, hemicellulose deposition and biomass porosity. These caused an integrative enhancement for biomass enzymatic saccharification and Cd accumulation in three mutants (Fig. 10). Therefore, this study has not only demonstrated pectin methylesterases catalysis for pectin methylation and plant cell wall network remodeling, but it has also provided a novel strategy for precise pectin modification to enhance biomass enzymatic saccharification and Cd phytoremediation in rice and beyond.

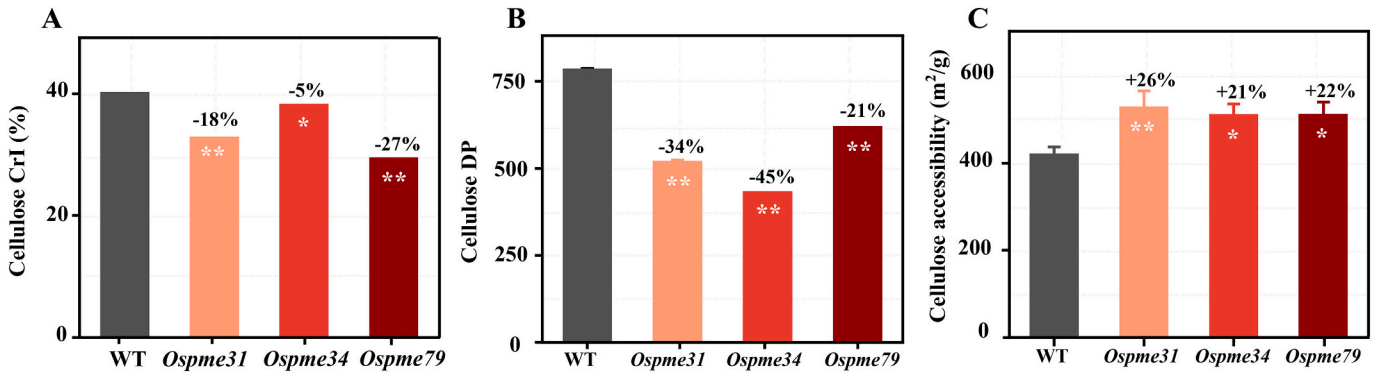

Fig. 7. Cellulose features of young seedlings in rice mutants and WT. (A, B) Cellulose crystalline index (CrI) and degree of polymerization (DP) of raw biomass; (C) Cellulose accessibility of 1 % NaOH-pretreated lignocellulose residues by Congo red staining; ** As significant difference by *t*-test between the mutant and WT at $p < 0.01$ levels (n = 3), respectively; [#] The percentage value calculated by subtraction between mutant and WT divided by WT. (For interpretation of the references to colour in this figure legend, the reader is referred to the web version of this article.)

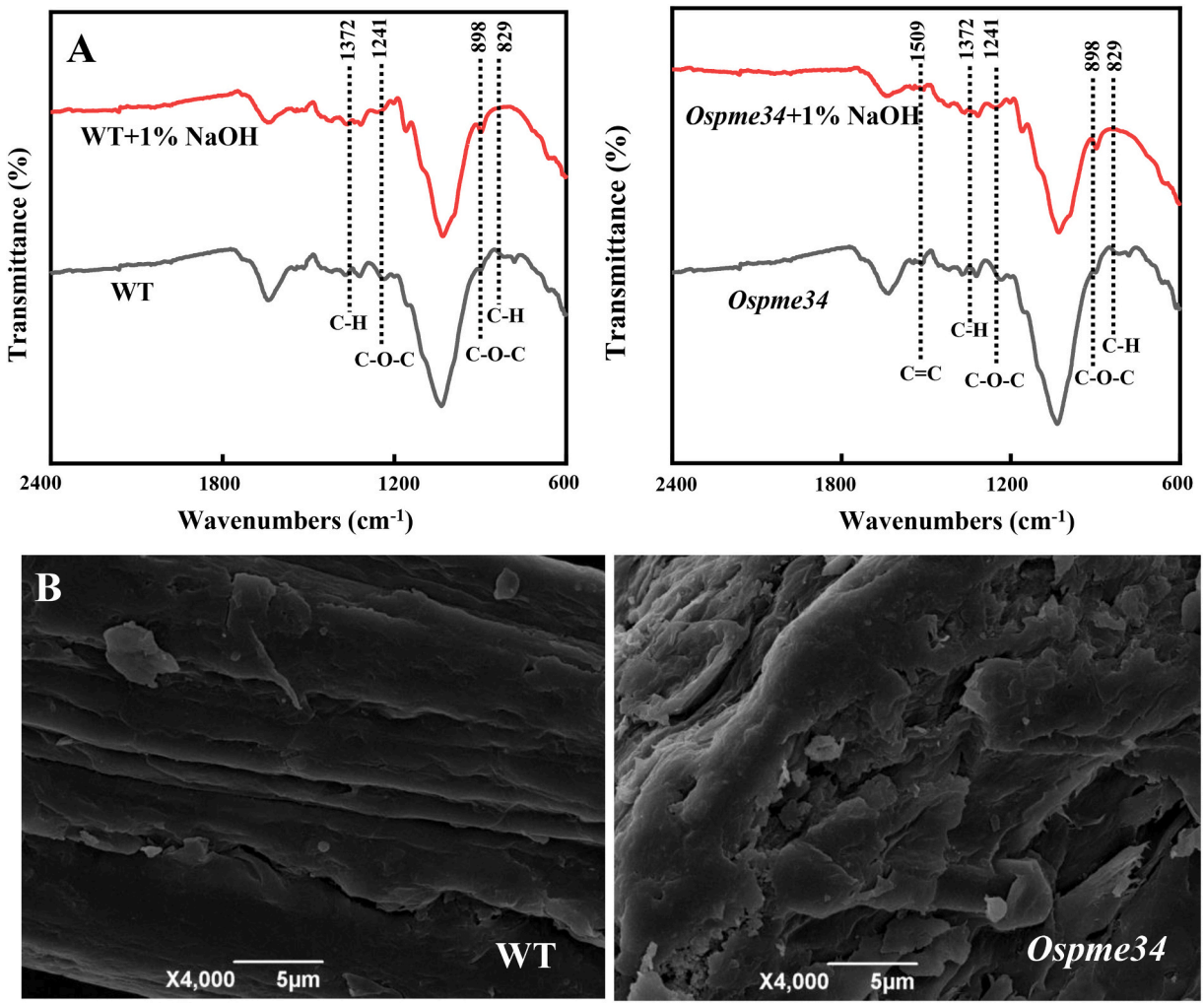

Fig. 8. Characterization of wall polymer interlinkages and lignocellulose surfaces with young seedlings in *Ospme34* mutants and WT. (A) FITR profiling for lignocelluloses after 1 % NaOH pretreatments as annotated in Table S2; (B) Scanning electron microscopy images for enzyme-undigestible residues after 1 % NaOH pretreatments.

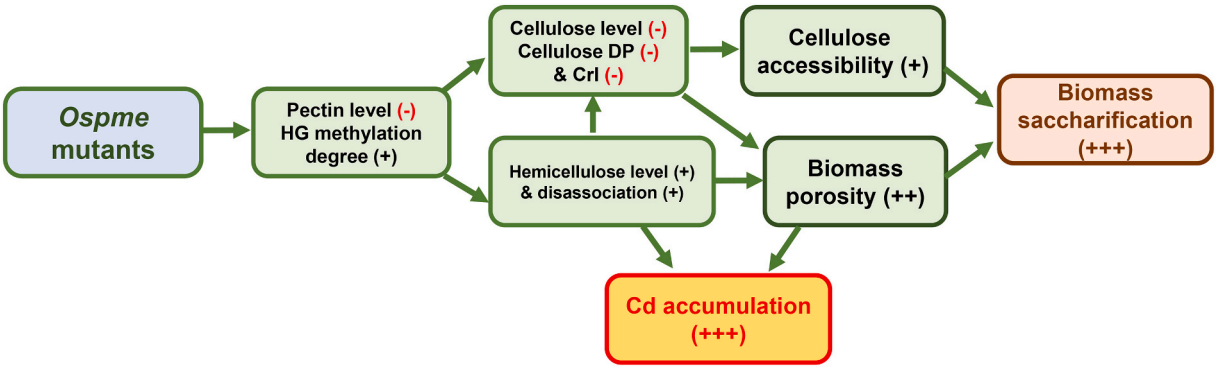

Fig. 9. A hypothetic model to elucidate how pectin methylation is upgraded for enhancing biomass enzymatic saccharification and Cd accumulation in three *Ospme* mutants. (+) And (−) as increased and decreased factors/parameters, respectively.

Author statement

The authors hereby solemnly promise that it did not use any artificial intelligence or AI-assisted technology during the preparation of this manuscript.

CRediT authorship contribution statement

Yanting Wang: Formal analysis, Investigation, Methodology, Writing – original draft. **Jiaxue Wen:** Formal analysis, Investigation, Validation. **Sufang Li:** Investigation, Methodology. **Jiaying Li:** Investigation, Methodology. **Hua Yu:** Formal analysis, Methodology. **Yunong Li:** Investigation. **Xifeng Ren:** Funding acquisition, Project

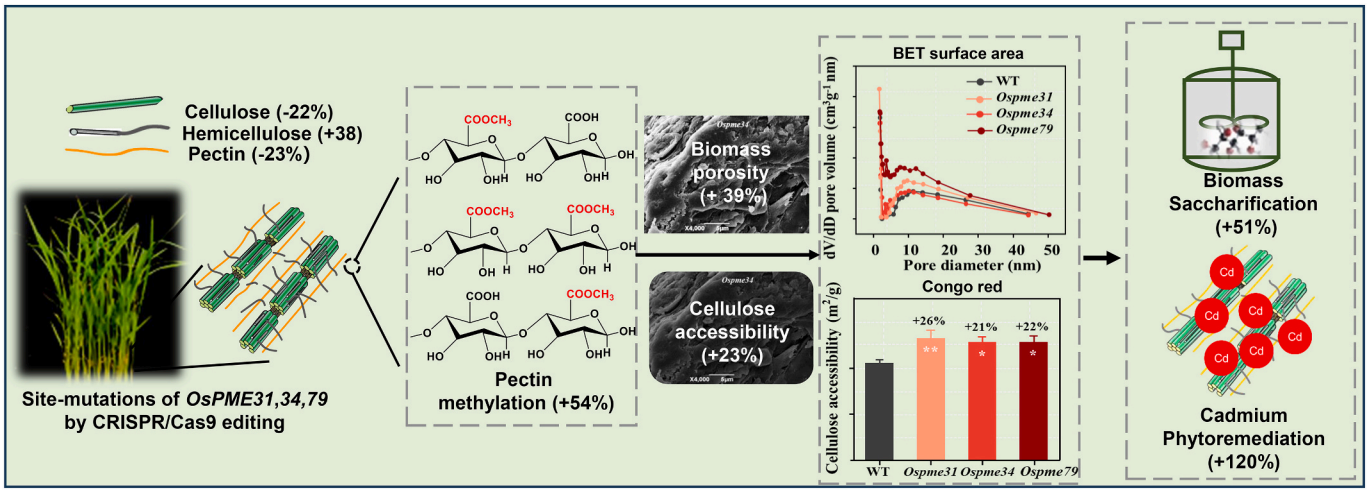

Fig. 10. A conclusion about rice *Ospmes* site-mutations for pectin methylation promotion to alter wall polysaccharide composition and to increase wall porosity and cellulose accessibility, leading to dual enhancements of biomass saccharification *in vitro* and Cd adsorption *in vivo*. All data about the increased/decreased rates (+/−%) were calculated by the average value of three mutants relative to the WT.

administration, Validation. **Lingqiang Wang:** Funding acquisition, Project administration, Validation. **Jingfeng Tang:** Funding acquisition, Project administration, Validation. **Xin Zhang:** Methodology. **Zhongqi Liu:** Funding acquisition, Project administration, Validation. **Liangcai Peng:** Conceptualization, Funding acquisition, Supervision, Writing – review & editing.

Declaration of competing interest

The authors have no conflicts of interest to declare.

Data availability

The authors do not have permission to share data.

Acknowledgments

This work was in part supported by the National Natural Science Foundation of China (32101701 to Y. W, 32170268 to L. P), National 111 Project of China (BP0820035 to L. P, D17009 to J. T), the Initiative Grant of Hubei University of Technology for High-level Talents (GCC20230001 to L. P).

Appendix A. Supplementary data

Supplementary data to this article can be found online at https://doi.org/10.1016/j.ijbiomac.2024.130137.

References

[1] Y. Wang, P. Liu, G. Zhang, Q. Yang, J. Lu, T. Xia, Cascading of engineered bioenergy plants and fungi sustainable for low-cost bioethanol and high-value biomaterials under green-like biomass processing, Renew. Sust. Energ. Rev. 137 (2021) 110586, https://doi.org/10.1016/j.rser.2020.110586.
[2] R. Zhang, Z. Hu, Y. Wang, H. Hu, F. Li, M. Li, Single-molecular insights into the breakpoint of cellulose nanofibers assembly during saccharification, Nat. Commun. 14 (2023) 1100, https://doi.org/10.1038/s41467-023-36856-8.
[3] M. Pauly, K. Keegstra, Cell-wall carbohydrates and their modification as a resource for biofuels, Plant J. 54 (2008) 559–568, https://doi.org/10.1111/j.1365-313X.2008.03463.x.
[4] Z. Li, L. Wu, C. Wang, Y. Wang, L. He, Z. Wang, Characterization of pectin methylesterase gene family and its possible role in juice sac granulation in navel orange (*Citrus sinensis Osbeck*), BMC Genomics 23 (2022) 185, https://doi.org/10.1186/s12864-022-08411-0.
[5] Z. Dang, Y. Wang, M. Wang, L. Cao, N. Ruan, Y. Huang, The fragile culm19 (FC19) mutation largely improves plant lodging resistance, biomass saccharification, and cadmium resistance by remodeling cell walls in rice, J. Hazard. Mater. 458 (2023) 132020, https://doi.org/10.1016/j.jhazmat.2023.132020.
[6] Y. Guo, S. Wang, K. Yu, H.-L. Wang, H. Xu, C. Song, Manipulating microRNA *miR408* enhances both biomass yield and saccharification efficiency in poplar, Nat. Commun. 14 (2023) 4285, https://doi.org/10.1038/s41467-023-39930-3.
[7] D. Mohnen, Pectin structure and biosynthesis, Curr. Opin. Plant Biol. 11 (2008) 266–277. doi:https://doi.org/10.1016/j.pbi.2008.03.006.
[8] K.T. Haas, R. Wightman, E.M. Meyerowitz, A. Peaucelle, Pectin homogalacturonan nanofilament expansion drives morphogenesis in plant epidermal cells, Science 367 (2020) 1003–1007, https://doi.org/10.1126/science.aaz5103.
[9] X. Liu, H. Cui, B. Zhang, M. Song, S. Chen, C. Xiao, Reduced pectin content of cell walls prevents stress-induced root cell elongation in Arabidopsis, J. Exp. Bot. 72 (2021) 1073–1084, https://doi.org/10.1093/jxb/eraa533.
[10] K.H. Caffall, D. Mohnen, The structure, function, and biosynthesis of plant cell wall pectic polysaccharides, Carbohydr. Res. 344 (2009) 1879–1900, https://doi.org/10.1016/j.carres.2009.05.021.
[11] G. De Lorenzo, S. Ferrari, M. Giovannoni, B. Mattei, F. Cervone, Cell wall traits that influence plant development, immunity, and bioconversion, Plant J. 97 (2019) 134–147, https://doi.org/10.1111/tpj.14196.
[12] L. Tan, S. Eberhard, S. Pattathil, C. Warder, J. Glushka, C. Yuan, An *Arabidopsis* cell wall proteoglycan consists of pectin and arabinoxylan covalently linked to an arabinogalactan protein, Plant Cell 25 (2013) 270–287, https://doi.org/10.1105/tpc.112.107334.
[13] R.P. Jolie, T. Duvetter, A.M. Van Loey, M.E. Hendrickx, Pectin methylesterase and its proteinaceous inhibitor: a review, Carbohydr. Res. 345 (2010) 2583–2595, https://doi.org/10.1016/j.carres.2010.10.002.
[14] H. Y. Jeong, H. P. Nguyen, C. Lee, Genome-wide identification and expression analysis of rice pectin methylesterases: implication of functional roles of pectin modification in rice physiology, J. Plant Physiol. 183 (2015) 23–29. doi:https://doi.org/10.1016/j.jplph.2015.05.001.
[15] H. Yu, M. Hu, Z. Hu, F. Liu, H. Yu, Q. Yang, Insights into pectin dominated enhancements for elimination of toxic Cd and dye coupled with ethanol production in desirable lignocelluloses, Carbohydr. Polym. 286 (2022) 119298, https://doi.org/10.1016/j.carbpol.2022.119298.
[16] R.-H. Liang, Y. Li, L. Huang, X.-D. Wang, X.-X. Hu, C.-M. Liu, Pb^{2+} adsorption by ethylenediamine-modified pectins and their adsorption mechanisms, Carbohydr. Polym. 234 (2020) 115911, https://doi.org/10.1016/j.carbpol.2020.115911.
[17] M. Celus, C. Kyomugasho, Z.J. Kermani, K. Roggen, A.M. Van Loey, T. Grauwet, Fe^{2+} adsorption on citrus pectin is influenced by the degree and pattern of methylesterification, Food Hydrocoll. 73 (2017) 101–109, https://doi.org/10.1016/j.foodhyd.2017.06.021.
[18] C. Xu, J. Zhu, H. Yu, H. Yu, Y. Yang, Q. Fu, Recyclable cascading of arsenic phytoremediation and lead removal coupled with high bioethanol production using desirable rice straws, Biochem. Eng. J. 168 (2021) 107950, https://doi.org/10.1016/j.bej.2021.107950.
[19] M. Madadi, Y. Wang, C. Xu, P. Liu, Y. Wang, T. Xia, Using *Amaranthus* green proteins as universal biosurfactant and biosorbent for effective enzymatic degradation of diverse lignocellulose residues and efficient multiple trace metals remediation of farming lands, J. Hazard. Mater. 406 (2021) 124727, https://doi.org/10.1016/j.jhazmat.2020.124727.
[20] Y. Wang, J. Huang, Y. Li, K. Xiong, Y. Wang, F. Li, Ammonium oxalate-extractable uronic acids positively affect biomass enzymatic digestibility by reducing lignocellulose crystallinity in *Miscanthus*, Bioresour. Technol. 196 (2015) 391–398, https://doi.org/10.1016/j.biortech.2015.07.099.
[21] S. Cheng, H. Yu, M. Hu, Y. Wu, L. Cheng, Q. Cai, *Miscanthus* accessions distinctively accumulate cadmium for largely enhanced biomass enzymatic saccharification by

increasing hemicellulose and pectin and reducing cellulose CrI and DP, Bioresour. Technol. 263 (2018) 67–74, https://doi.org/10.1016/j.biortech.2018.04.031.
[22] Y. Zhang, C. Xu, J. Lu, H. Yu, J. Zhu, J. Zhou, An effective strategy for dual enhancements on bioethanol production and trace metal removal using *Miscanthus* straws, Ind. Crop. Prod. 152 (2020) 112393, https://doi.org/10.1016/j.indcrop.2020.112393.
[23] Y. Wu, M. Wang, L. Yu, S.-W. Tang, T. Xia, H. Kang, A mechanism for efficient cadmium phytoremediation and high bioethanol production by combined mild chemical pretreatments with desirable rapeseed stalks, Sci. Total Environ. 708 (2020) 135096, https://doi.org/10.1016/j.scitotenv.2019.135096.
[24] C. Wang, W. Guo, X. Cai, R. Li, D. W. Ow, Engineering low-cadmium rice through stress-inducible expression of OXS3-family member genes, New Biotechnol. 48 (2019) 29–34. doi:https://doi.org/10.1016/j.nbt.2018.04.004.
[25] C. Lu, L. Zhang, Z. Tang, X.-Y. Huang, J.F. Ma, F.-J. Zhao, Producing cadmium-free *Indica* rice by overexpressing *OsHMA3*, Environ. Int. 126 (2019) 619–626, https://doi.org/10.1016/j.envint.2019.03.004.
[26] X. Guo, Y. Liu, R. Zhang, J. Luo, Y. Song, J. Li, Hemicellulose modification promotes cadmium hyperaccumulation by decreasing its retention on roots in *Sedum alfredii*, Plant Soil 447 (2020) 241–255, https://doi.org/10.1007/s11104-019-04339-9.
[27] Z. Shao, J. Lu, J. Ding, F. Fan, X. Sun, P. Li, Novel green chitosan-pectin gel beads for the removal of Cu(II), Cd(II), Hg(II) and Pb(II) from aqueous solution, Int. J. Biol. Macromol. 176 (2021) 217–225. doi:https://doi.org/10.1016/j.ijbiomac.2021.02.037.
[28] M.A. Ismael, A.M. Elyamine, M.G. Moussa, M. Cai, X. Zhao, C. Hu, Cadmium in plants: uptake, toxicity, and its interactions with selenium fertilizers, Metallomics 11 (2019) 255–277, https://doi.org/10.1039/c8mt00247a.
[29] Z. Li, X. Zhang, C. Zhu, Physicochemical properties and Pb^{2+} adsorption capacity of freeze-dried hawthorn pectin fractions by gradient ethanol precipitation, Int. J. Biol. Macromol. 245 (2023) 125581, https://doi.org/10.1016/j.ijbiomac.2023.125581.
[30] Y. Li, J. Zhuo, P. Liu, P. Chen, H. Hu, Y. Wang, Distinct wall polymer deconstruction for high biomass digestibility under chemical pretreatment in *Miscanthus* and rice, Carbohydr. Polym. 192 (2018) 273–281, https://doi.org/10.1016/j.carbpol.2018.03.013.
[31] M. Li, J. Wang, Y. Yang, G. Xie, Alkali-based pretreatments distinctively extract lignin and pectin for enhancing biomass saccharification by altering cellulose features in sugar-rich Jerusalem artichoke stem, Bioresour. Technol. 208 (2016) 31–41. doi:https://doi.org/10.1016/j.biortech.2016.02.053.
[32] L. Wu, S. Feng, J. Deng, B. Yu, Y. Wang, B. He, Altered carbon assimilation and cellulose accessibility to maximize bioethanol yield under low-cost biomass processing in corn brittle stalk, Green Chem. 21 (2019) 4388–4399, https://doi.org/10.1039/C9GC01237K.
[33] Z. Wu, K. Peng, Y. Zhang, M. Wang, C. Yong, L. Chen, Lignocellulose dissociation with biological pretreatment towards the biochemical platform: a review, Mater. Today Bio. 16 (2022) 100445, https://doi.org/10.1016/j.mtbio.2022.100445.
[34] H. Gao, Y. Wang, Q. Yang, H. Peng, Y. Li, D. Zhan, Combined steam explosion and optimized green-liquor pretreatments are effective for complete saccharification to maximize bioethanol production by reducing lignocellulose recalcitrance in one-year-old bamboo, Renew. Energy 175 (2021) 1069–1079, https://doi.org/10.1016/j.renene.2021.05.016.
[35] S. Baramee, A.-K. Siriatcharanon, P. Ketbot, T. Teeravivattanakit, R. Waeonukul, P. Pason, Biological pretreatment of rice straw with cellulase-free xylanolytic enzyme-producing *Bacillus firmus* K-1: structural modification and biomass digestibility, Renew. Energy 160 (2020) 555–563, https://doi.org/10.1016/j.renene.2020.06.061.
[36] A. Abraham, A.K. Mathew, R. Sindhu, A. Pandey, P. Binod, Potential of rice straw for bio-refining: an overview, Bioresour. Technol. 215 (2016) 29–36, https://doi.org/10.1016/j.biortech.2016.04.011.
[37] T.L. Bailey, N. Williams, C. Misleh, W.W. Li, MEME: discovering and analyzing DNA and protein sequence motifs, Nucleic Acids Res. 34 (2006) W369–W373, https://doi.org/10.1093/nar/gkl198.
[38] Z. Hu, H. Peng, J. Liu, H. Zhang, S. Li, H. Wang, Integrating genetic-engineered cellulose nanofibrils of rice straw with mild chemical treatments for enhanced bioethanol conversion and bioaerogels production, Ind. Crop. Prod. 202 (2023) 117044, https://doi.org/10.1016/j.indcrop.2023.117044.
[39] G. Zhang, L. Wang, X. Li, S. Bai, Y. Xue, Z. Li, Distinctively altered lignin biosynthesis by site-modification of OsCAD2 for enhanced biomass saccharification in rice, GCB Bioenergy 13 (2021) 305–319, https://doi.org/10.1111/gcbb.12772.
[40] I.O. Saheed, E.N.M. Yusof, W.-D. Oh, M.A.K.M. Hanafiah, F.B.M. Suah, Fabrication of chitosan@activated carbon composites in EmimAc for Cd(II) adsorption from aqueous solution: experimental, optimization and DFT study, Int. J. Biol. Macromol. 242 (2023) 124798, https://doi.org/10.1016/j.ijbiomac.2023.124798.
[41] P. Liu, A. Li, Y. Wang, Q. Cai, H. Yu, Y. Li, Distinct *Miscanthus* lignocellulose improves fungus secreting cellulases and xylanases for consistently enhanced biomass saccharification of diverse bioenergy crops, Renew. Energy 174 (2021) 799–809, https://doi.org/10.1016/j.renene.2021.04.107.
[42] J. Jia, B. Yu, L. Wu, H. Wang, Z. Wu, M. Li, Biomass enzymatic saccharification is determined by the non-KOH-extractable wall polymer features that predominately affect cellulose crystallinity in corn, PLoS One 9 (2014) e108449, https://doi.org/10.1371/journal.pone.0108449.
[43] Z. Wu, H. Hao, Y. Zahoor, Z. Tu, F. Wei Hu, Diverse cell wall composition and varied biomass digestibility in wheat straw for bioenergy feedstock, Biomass Bioenergy 70 (2014) 347–355, https://doi.org/10.1016/j.biombioe.2014.08.025.
[44] H. Hu, R. Zhang, Z. Tao, X. Li, Y. Li, J. Huang, Cellulose synthase mutants distinctively affect cell growth and cell wall integrity for plant biomass production in *Arabidopsis*, Plant Cell Physiol. 59 (2018) 1144–1157, https://doi.org/10.1093/pcp/pcy050.
[45] H. Peng, W. Zhao, J. Liu, P. Liu, H. Yu, J. Deng, Distinct cellulose nanofibrils generated for improved Pickering emulsions and lignocellulose-degradation enzyme secretion coupled with high bioethanol production in natural rice mutants, Green Chem. 24 (2022) 2975–2987, https://doi.org/10.1039/D1GC04447H.
[46] M. Wiman, D. Dienes, M.A.T. Hansen, T. van der Meulen, G. Zacchi, G. Lidén, Cellulose accessibility determines the rate of enzymatic hydrolysis of steam-pretreated spruce, Bioresour. Technol. 126 (2012) 208–215, https://doi.org/10.1016/j.biortech.2012.08.082.
[47] Y. Chen, C. Ma, W. Tang, Y.-C. He, Comprehensive understanding of enzymatic saccharification of betaine: lactic acid-pretreated sugarcane bagasse, Bioresour. Technol. 386 (2023) 129485, https://doi.org/10.1016/j.biortech.2023.129485.
[48] Y. Li, H. Sun, C. Fan, H. Hu, L. Wu, X. Jin, Overproduction of fungal endo-β-1,4-glucanase leads to characteristic lignocellulose modification for considerably enhanced biomass enzymatic saccharification and bioethanol production in transgenic rice straw, Cellulose 26 (2019) 8249–8261, https://doi.org/10.1007/s10570-019-02500-2.
[49] C. Fan, H. Yu, S. Qin, Y. Li, A. Alam, C. Xu, Brassinosteroid overproduction improves lignocellulose quantity and quality to maximize bioethanol yield under green-like biomass process in transgenic poplar, Biotechnol. Biofuels 13 (2020) 7, https://doi.org/10.1186/s13068-020-1652-z.
[50] R. Zhang, Z. Hu, H. Peng, P. Liu, Y. Wang, J. Li, High density cellulose nanofibril assembly leads to upgraded enzymatic and chemical catalysis of fermentable sugars, cellulose nanocrystals and cellulase production by precisely engineering cellulose synthase complexes, Green Chem. 25 (2023) 1096–1106, https://doi.org/10.1039/D2GC03744K.
[51] G. De Lorenzo, S. Ferrari, M. Giovannoni, B. Mattei, F. Cervone, Cell wall traits that influence plant development, immunity, and bioconversion, Plant J. 97 (2019) 134–147. doi:https://doi.org/10.1111/tpj.14196.
[52] S. V. Popov, Y. S. Ovodov, Polypotency of the immunomodulatory effect of pectins, Biochem. Biokhimiia. 78 (2013) 823–835. doi:https://doi.org/10.1134/s0006297913070134.
[53] T.V. Komarova, E.V. Sheshukova, Y.L. Dorokhov, Cell wall methanol as a signal in plant immunity, Front. Plant Sci. 5 (2014) 101, https://doi.org/10.3389/fpls.2014.00101.
[54] E. Bonnin, C. Alvarado, M.J. Crépeau, B. Bouchet, C. Garnier, F. Jamme, Mobility of pectin methylesterase in pectin/cellulose gels is enhanced by the presence of cellulose and by its catalytic capacity, Sci. Rep. 9 (2019) 12551, https://doi.org/10.1038/s41598-019-49108-x.
[55] Z. Hu, Q. Li, Y. Chen, T. Li, Y. Wang, R. Zhang, Intermittent ultrasound retains cellulases unlock for enhanced cellulosic ethanol with high-porosity biochar for dye adsorption using desirable rice mutant straw, Bioresour. Technol. 369 (2023) 128437, https://doi.org/10.1016/j.biortech.2022.128437.
[56] N. Carpita, D. Sabularse, D. Montezinos, D.P. Delmer, Determination of the pore size of cell walls of living plant cells, Science 205 (1979) 1144–1147, https://doi.org/10.1126/science.205.4411.1144.
[57] Y. Gao, A.S. Lipton, C.R. Munson, Y. Ma, K.L. Johnson, D.T. Murray, Elongated galactan side chains mediate cellulose–pectin interactions in engineered *Arabidopsis* secondary cell walls, Plant J. 115 (2023) 529–545, https://doi.org/10.1111/tpj.16242.
[58] Y. Fu, H. Gao, H. Yu, Q. Yang, H. Peng, P. Liu, Specific lignin and cellulose depolymerization of sugarcane bagasse for maximum bioethanol production under optimal chemical fertilizer pretreatment with hemicellulose retention and liquid recycling, Renew. Energy 200 (2022) 1371–1381, https://doi.org/10.1016/j.renene.2022.10.049.
[59] J. Du, C.T. Anderson, C. Xiao, Dynamics of pectic homogalacturonan in cellular morphogenesis and adhesion, wall integrity sensing and plant development, Nat. Plants 8 (2022) 332–340, https://doi.org/10.1038/s41477-022-01120-2.
[60] L.D. Fernando, W. Zhao, I. Gautam, A. Ankur, T. Wang, Polysaccharide assemblies in fungal and plant cell walls explored by solid-state NMR, Structure 31 (2023) 1375–1385, https://doi.org/10.1016/j.str.2023.07.012.
[61] P. Phyo, T. Wang, C. Xiao, C.T. Anderson, M. Hong, Effects of pectin molecular weight changes on the structure, dynamics, and polysaccharide interactions of primary cell walls of *Arabidopsis thaliana*: insights from solid-state NMR, Biomacromolecules 18 (2017) 2937–2950, https://doi.org/10.1021/acs.biomac.7b00888.
[62] A. Kirui, J. Du, W. Zhao, W. Barnes, X. Kang, C.T. Anderson, A pectin methyltransferase modulates polysaccharide dynamics and interactions in *Arabidopsis* primary cell walls: evidence from solid-state NMR, Carbohydr. Polym. 270 (2021) 118370, https://doi.org/10.1016/j.carbpol.2021.118370.
[63] T. Wang, M. Hong, Solid-state NMR investigations of cellulose structure and interactions with matrix polysaccharides in plant primary cell walls, Ind. Crop. Prod. 67 (2015) 503–514, https://doi.org/10.1093/jxb/erv416.
[64] G.D. Strahan, A.T. Hotchkiss, S. Dieng, J. Hirsch, 1D and 2D NMR datasets, resonance assignments and coupling constant analysis of red beet fiber and pectin, Data Brief 46 (2023) 108845, https://doi.org/10.1016/j.dib.2022.108845.